



Enzymes immobilized on amine-terminated ionic liquid-functionalized carbon nanotube for hydrogen peroxide determination

Xiuhui Liu*, Caihong Bu, Zhihan Nan, Lichun Zheng, Yu Qiu, Xiaoquan Lu**

Key Laboratory of Bioelectrochemistry & Environmental Analysis of Gansu Province, College of Chemistry & Chemical Engineering, Northwest Normal University, No. 967 Anning East Road, Lanzhou, Gansu 730070, PR China

ARTICLE INFO

Article history:

Received 17 July 2012

Received in revised form

18 November 2012

Accepted 24 November 2012

Available online 1 December 2012

Keywords:

Functionalization of carbon nanotube

Ionic liquid

Hydrogen peroxide

Cytochrome C

Amperometry

ABSTRACT

We report on a new approach for the electrochemical detection of hydrogen peroxide (H_2O_2) based on Cytochrome C (Cyt c) immobilized ionic liquid (IL)-functionalized multi-walled carbon nanotubes (MWCNTs) modified glass carbon electrode (GCE). Functionalization of multi-walled carbon nanotube with amine-terminated ionic liquid materials was characterized using Fourier transform infrared spectroscopy (FTIR), UV–vis spectra, and electrochemical impedance spectroscopy (EIS), and the results showed that the covalent modification of MWCNTs with ILs exhibited a high surface area for enzyme immobilization and provided a good microenvironment for Cyt c to retain its bioelectrocatalytic activity toward H_2O_2 . Amperometry was used to evaluate the catalytic activity of the Cyt c towards H_2O_2 . The proposed biosensor exhibited a wide linear response range nearly 4 orders of magnitude of H_2O_2 ($4.0 \times 10^{-8} \text{ M}$ – $1.0 \times 10^{-4} \text{ M}$) with a good linearity (0.9980) and a low detection limit of $1.3 \times 10^{-8} \text{ M}$ (based on $S/N=3$). Furthermore, the biosensor also displays some other excellent characteristics such as high selectivity, good reproducibility and long-term stability. Thus, the biosensor constructed in this study has great potential for detecting H_2O_2 in the complex biosystems.

© 2012 Elsevier B.V. All rights reserved.

1. Introduction

Hydrogen peroxide (H_2O_2) is a reactive oxygen species (ROS) and a by-product of several oxidative metabolic pathways [1]. The relationship between H_2O_2 concentration and human health has attracted great attention [2], and the determination of H_2O_2 is of practical importance in clinical, environmental, and industrial research. For this reason there has been an increasing interest in the design of reliable H_2O_2 sensors. A number of sensors have been fabricated to determine H_2O_2 [3–8]. In particular, as biocatalysts, enzymes have a high substrate specificity and reactive efficiency under ambient conditions compared to artificial inorganic catalysts. Nevertheless, the harsh conditions required for chemical reactions limit their applicability because it is difficult to maintain their highly complex molecular configurations [9]. Therefore, a useful strategy to overcome these limitations is to find conductive materials with good biocompatibility.

Carbon nanotubes (CNTs) have been considered as an important class of nanomaterials with outstanding electronic, chemical, and mechanical properties since its discovery in 1991 by Iijima [10].

Recently, a number of research groups have focused on the chemical modification of CNTs through covalent or noncovalent functionalizations [11–16]. These functionalized CNTs modified electrodes exhibited stable electrocatalytic responses towards many important biomolecules such as nicotinamide adenine dinucleotide (NADH) [17], ascorbic acid (AA), dopamine (DA) [18] and cytochrome C (Cyt c) [19]. In addition, many researches focused on CNTs-enzyme-based biosensor [20–22] because CNTs can maintain the bioactivity of enzymes and improve the sensitivity of sensors. However, the major barrier is that coating of the CNTs with an enzyme layer tends to block the electron transport pathway [23] and causes poor dispersion on the CNT surfaces [24], which may greatly limit their application in biosensor systems.

It is widely accepted that the successful synthesis of ILs and CNTs has been proved to be a recent breakthrough in interdisciplinary research because of the unique properties and the striking applications of both kinds of materials [25]. As we know that most biomolecules are charged in biological environments, therefore, IL functionalization of CNTs would provide an alternative method to easily immobilize biomolecules for detection. However, the related studies were few [26,23]. For CNT-based biosensors, there are still some developmental challenges to be addressed. Herein we report our finding that the covalent modification of multiwalled carbon nanotubes (MWCNTs) with imidazolium salt-based ILs provided a good microenvironment

* Corresponding author. Tel.: +86 931 7975276; fax: +86 931 7971323.

** Corresponding author. Tel.: +86 931 7971276; fax: +86 931 7971323.

E-mail addresses: liuxh@nwnu.edu.cn, liuyr1008@sina.com.cn (X. Liu), liuxq@nwnu.edu.cn (X. Lu).

for HRP or Cyt c to retain their bioelectrocatalytic activity toward H_2O_2 .

2. Experimental

2.1. Reagents

The multi-walled carbon nanotubes (MWNTs) used (diameter: 20–40 nm, length: 1–2 μm , purity: $\geq 95\%$) came from Shenzhen Nanotech Port Co., Ltd. (Shenzhen, China). HRP ($> 160 \text{ IU mg}^{-1}$) was from Sigma (USA), and Cyt c came from Shanghai Yuanye biological Co. Ltd (Shanghai, China). Hydrogen peroxide solution (30 wt%) was purchased from Beijing Chemical Reagent (Beijing, China). Bromopropylamine and 1-methylimidazole were obtained from Acros (Beijing, China). And before use, 1-methylimidazole was distilled. PBS (pH 7.0) was prepared by mixing suitable amounts of 0.1 M $\text{NaH}_2\text{PO}_4/\text{Na}_2\text{HPO}_4$. Other chemicals were all of analytical grade, and the solutions were prepared by doubly distilled water.

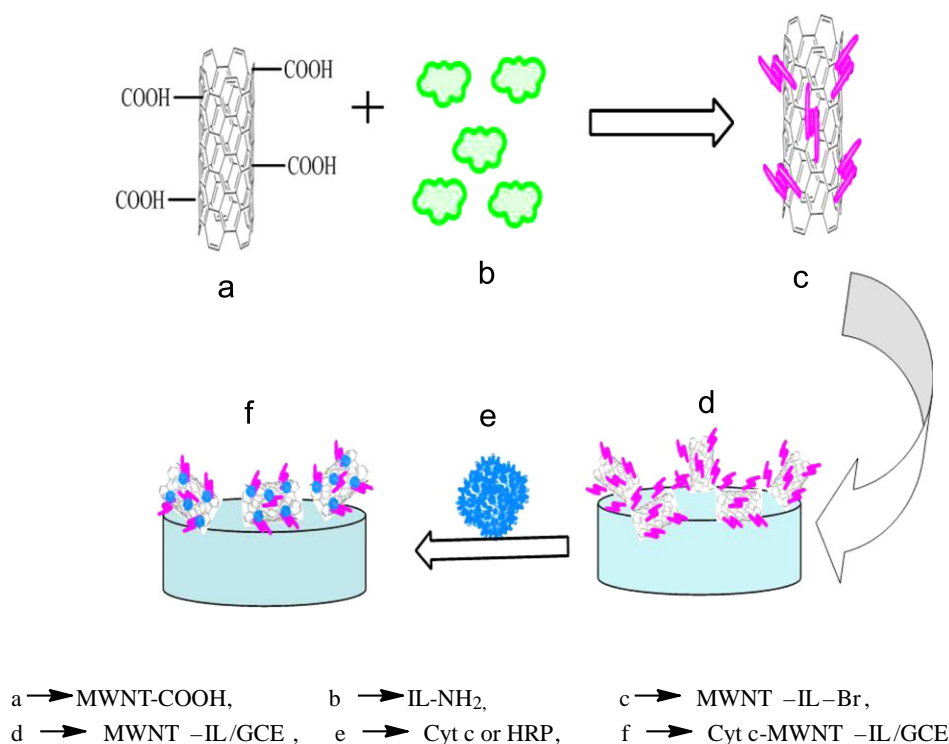
2.2. Instruments

Amperometric $i-t$ curve, cyclic voltammetric (CV) measurements were performed in a conventional three electrodes cell with a platinum wire as the auxiliary electrode and a saturated calomel electrode (SCE) as the reference electrode with a CHI 660c Electrochemical Workstation (Shanghai Chenhua Co., China). UV–vis absorption spectra were taken by absorption mode with a UV-1102 UV–vis spectrophotometer (Shanghai, China). Electrochemical impedance spectroscopy (EIS) experiments were performed on Multi-potentiostat (VMP2, Princeton Applied Research, USA). The working electrode was bare or modified glassy carbon electrode (GCE, $d=3.5 \text{ mm}$). All potentials given in this paper were

referred to the SCE. Before using, GCE was polished carefully with 0.3, and 0.05 μm alumina slurry to a mirror finish.

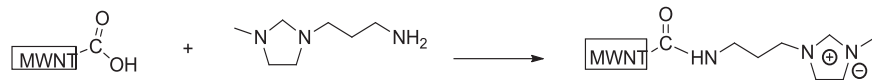
2.3. Preparation of Cyt c-MWNT-IL-modified GCE

IL functionalized MWNT (MWNT-IL-Br) was prepared by previously reported method [27]. In general, it was based on an amidation between carboxylic acid functionalized MWNT (MWNT-COOH) and the amine-terminated IL (1-propyl-amine-3-methylimidazolium bromide, IL-NH₂). The IL-NH₂ was prepared by the reaction of 1-methylimidazole (0.02 mol) with 3-bromo-propylamine (0.02 mol) in 50 mL ethanol under reflux in N_2 atmosphere for 24 h, the ethanol is removed in vacuo and the solid residue dissolved in a minimal quantity of water that is brought to pH 8 by the addition, in small portions, of solid KOH. The product imidazolium bromide is then separated from the KBr byproduct by evaporation of the water, followed by extraction of the residue with ethanol-THF, in which the imidazolium salt is soluble. FTIR verifies the structure and composition of the new IL [28]. MWNT-COOH was prepared by reflux the as-received MWNT in 3 M HCl and H_2O_2 . MWNT-IL was prepared by ultrasonically a solution of 5 mg of the MWNT-COOH, 10 mg of IL-NH₂, and 10 mg of dicyclohexylcarbodiimide (DCC) in 10 mL of dimethylformamide (DMF) for 15 min, and then vigorously stirring at 50 $^\circ\text{C}$ for 24 h. Then, unreacted MWNTs were removed by centrifuging. After that MWNT-IL-Br was filtered by nylon membrane with 0.22 μm pores, thoroughly washed with DMF, ethanol and water, separately. Then 18 μL of MWNT-IL-Br aqueous solution (0.05 mg/mL) was dropped on the surface of a GCE. After being dried in air for 24 h, MWNT-IL-Br modified GCE (GCE/MWNT-IL-Br) was thus obtained. Moreover, MWNT-IL-Br modified electrode was immersed in Cyt c solution (1 mg/mL, pH 7.0 PBS) for 2 h at 4 $^\circ\text{C}$. Then Cyt c was immobilized onto the surface of IL-nanohybrid film to form Cyt c-MWNTs-IL/GCE.



Scheme 1. Preparation of Cyt c-MWNT-IL-modified GCE.

The HRP/MWNTs-IL/GCE was prepared via the same method (Scheme 1).



3. Results and discussion

3.1. Characterization of MWNTs-IL materials

The method for IL functionalized MWNTs is depicted in Scheme 1, and the reaction is shown in the following:

First, UV–vis spectroscopic analysis, Fourier transform infrared spectroscopy (FTIR) analysis were used to confirm the reaction occurrence between MWNT and amine-terminated IL, as well as the presence of acid amide groups.

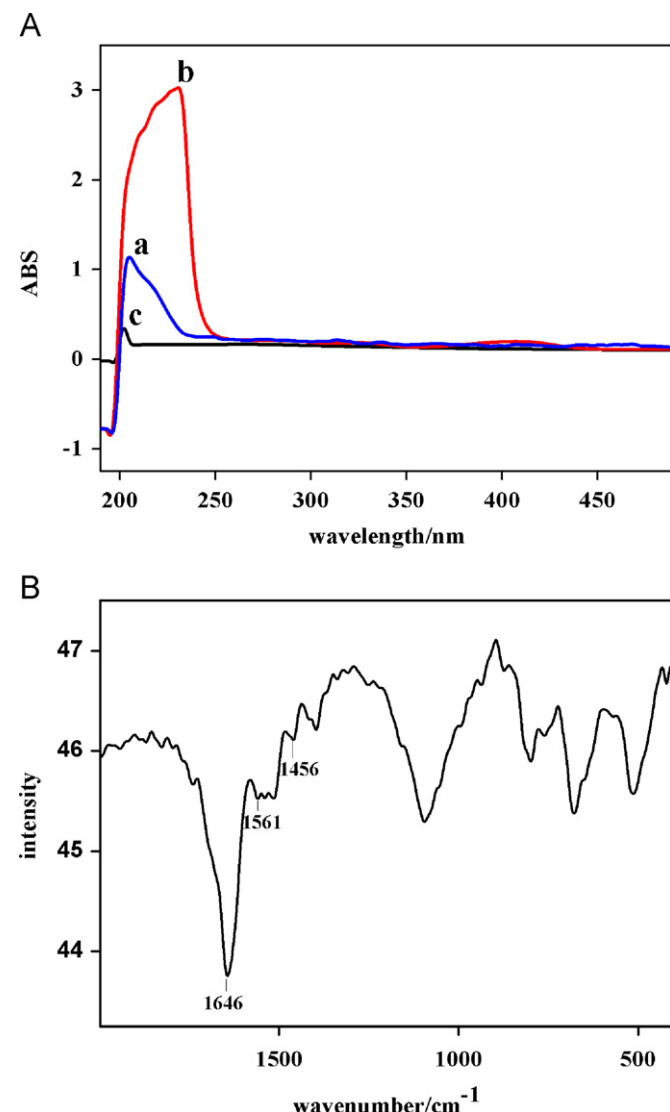


Fig. 1. (A) UV–vis spectral characterizations of (a) MWNTs-IL, (b) IL and (c) MWNTs in 0.1 M PBS (pH 7.0). (B) FT-IR spectra of MWNTs-IL.

Fig. 1A shows UV–vis spectroscopic analysis of MWNTs-IL, and the position of the absorption band may provide information about possible denaturation of MWNTs-IL. Compared to curve b where IL shows a maximum absorption at 230 nm, the MWNTs-IL (curve a) has an obvious blue shift (206 nm) of the solet absorption band and the absorbance of the peak decreased a lot.

The results indicated that the interaction between MWNT-COOH and IL-NH₂ had taken place and formed O=C–NH [29].

The acid amide groups were further characterized by Fourier transform infrared spectroscopy (FTIR) analysis as shown in Fig. 1B. The C=O band, which should appear at 1709 cm^{−1} according to Ref. [30], shifted to 1646 cm^{−1} due to the involvement of imidazole and carboxylic groups in the hydrogen bond [31], indicating the formation of the amide bond. In addition, the appearance of a peak at 1456 cm^{−1} provides strong evidence of forming the amide linkage between MWNT-COOH and IL-NH₂ [32]. This result was in accordance with the above result of the UV–vis analysis.

In addition, the electrochemical behaviors of different electrodes were studied with K₃Fe(CN)₆ as electroactive probe by cyclic voltammetry as shown in Fig. 2. At bare GCE (curve a), a reversible electrochemical response was observed at a potential of about 0.26 V with a peak-to-peak separation (ΔE_p) of 69 mV. After accumulation of MWNTs on the bare GCE (curve b), the peak current decreased deeply, which means the MWNTs would hinder the electron transfer from K₃Fe(CN)₆ to the electrode surface. In contrast, both the cathodic and anodic peak currents increased obviously as MWNTs-IL immobilized on the electrode surface (curve c). The oxidation current of MWNTs-IL (i_{pa} = 99.38 μ A) on the electrode is two times higher than that on the MWNTs/GCE (i_{pa} = 46.47 μ A). It revealed that the IL could detach the MWNTs from the bundles, and the synergistic effect of MWNTs and IL enhanced the conductivity effectively [33].

3.2. Characterization of immobilized Cyt c on MWNT-IL/GCE

It is well known that electrochemical impedance spectroscopy is an effective method to study the interface properties of surface-modified electrodes. The typical impedance spectrum includes a semicircle portion at higher frequencies corresponding to the

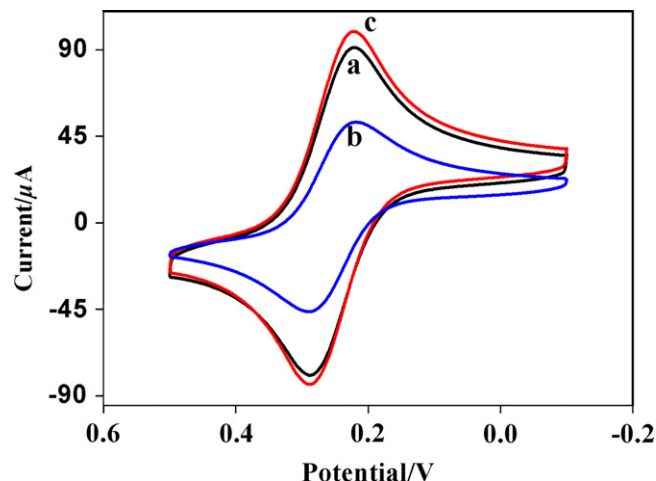


Fig. 2. Cyclic voltammograms of (a) bare GCE, (b) MWNTs/GCE, (c) MWNTs-IL/GCE in 5.0 mM K₃Fe(CN)₆ and 0.1 M KCl at a scan rate of 0.05 V s^{−1}.

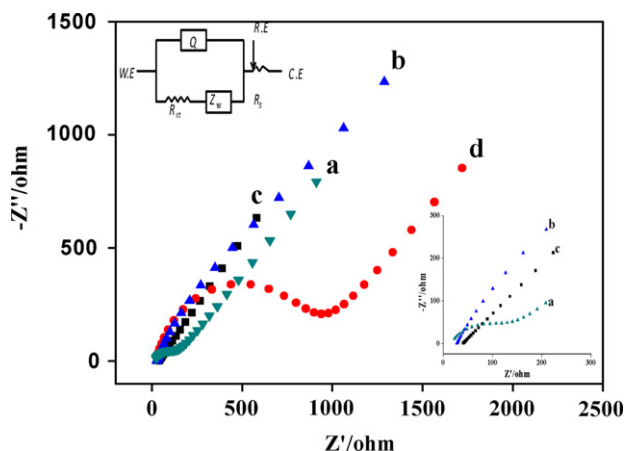


Fig. 3. EIS of (a) bare GCE, (b) MWNTs-IL/GCE, (c) Cyt c/MWNTs-IL/GCE, (d) Cyt c/GC in 5.0 mM $K_3Fe(CN)_6$ and 0.1 M KCl.

electron transfer-limited process and a linear part at lower frequency range representing the diffusion limited process. The semicircle diameter in the impedance spectrum equals the electron-transfer resistance, R_{et} . This resistance controls the electron-transfer kinetics of the redox probe at the electrode interface. Therefore, R_{et} can be used to describe the interface properties of the modified electrode. Its value varies when different substances are adsorbed on the electrode surface.

Using $[Fe(CN)_6]^{3-/4-}$ redox couples as the electrochemical probe, the EIS plots of different modified electrodes are shown in Fig. 3, and the inset shows the fits of equivalent circuit. When the GCE electrode surface was coated by Cyt c film, the R_{et} value of curve d increased to about 835 Ω , which manifested that Cyt c was adsorbed on the electrode surface, and the Cyt c film generated an obstruction to the electron transfer of the electrochemical probe at the electrode surface. However, when the MWNTs-IL modified the surface of GCE electrode, the diameter of the high frequency semicircle was significantly reduced to an almost straight tail line with a R_{et} value of 20 Ω as shown in Fig. 3 curve b. After that, with the Cyt c adsorbed on MWNTs-IL/GCE (curve c), R_{et} increased a little bit, and it might be caused by the hindrance of the macromolecular structure of Cyt c to the electron transfer. Thus, above results could clearly confirm that the IL functionalized MWNT effectively enhanced the conductivity of the modified electrode, and Cyt c was successfully immobilized on its surface.

Previous report has pointed out that Cyt c could physically absorb on the surface of MWNT weakly [28] because MWNT-COOH was negatively charged, and the electrostatic repulsion was against the physical absorption of Cyt c. But in this work, the IL-NH₂ (imidazolium cation) was positively charged, and was in favor of conjugation of negatively charged Cyt c. Moreover, Br⁻ anion in MWNT-IL-Br was ready to be exchanged by Cyt c when the MWNT-IL-Br modified electrode was immersed in Cyt c solution [25]. Therefore, IL functionalized MWNT material might provide an extra ionic affinity between MWNT and Cyt c, which is helpful for enzyme loading on the modified electrode.

It is very important to keep the bioactivity of Cyt c in MWNT-IL experimental system. The shape and position of the sorb absorption band of Cyt c can provide the structural information about Cyt c, especially about heme groups. Fig. S-1 showed UV-vis absorption spectra of Cyt c aqueous solution in the absence and presence of MWNTs-IL. One can see that no obvious peak shift at 409 nm (a heme band) in Fig. S-1a and b, indicating that Cyt c could keep its natural structure and bioactivity in PBS (pH 7.0).

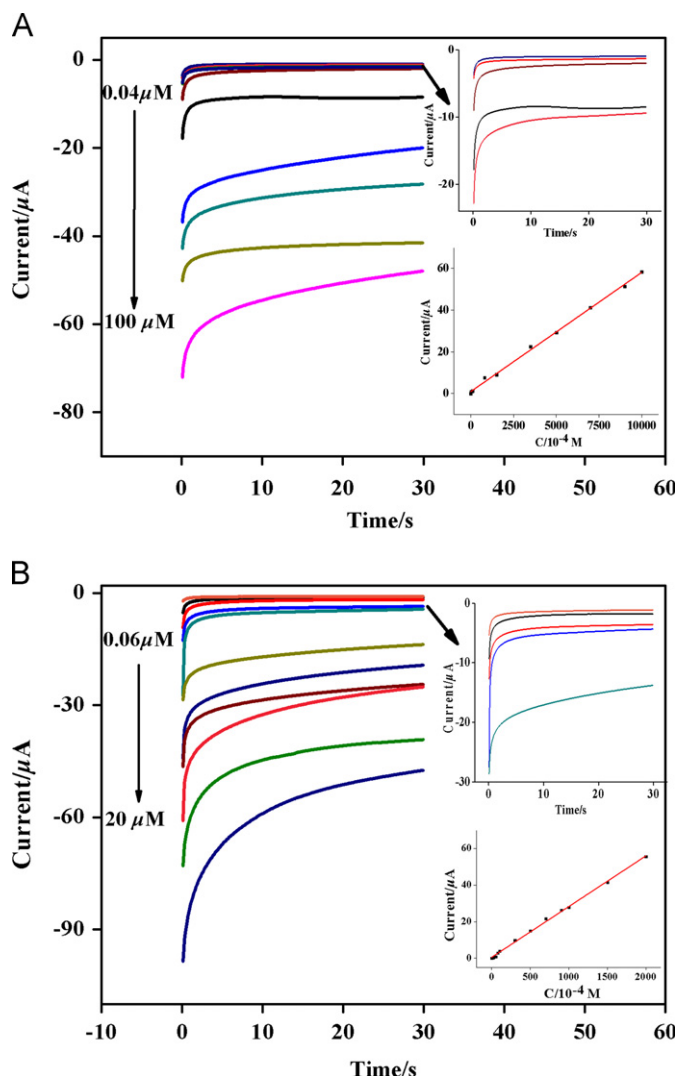
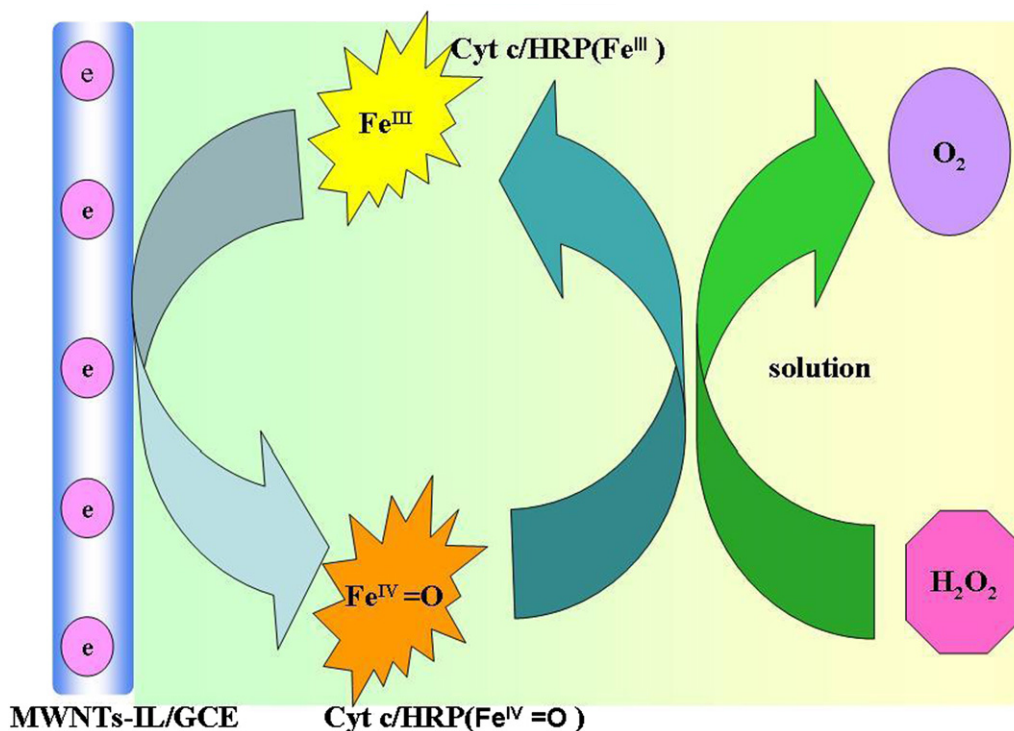


Fig. 4. (A) The chronoamperometry current-time curve of Cyt c-MWNT-IL/GCE with successive addition of 0.04, 0.1, 1, 15, 35, 50, 90 and 100 μ M H_2O_2 to 0.10 M pH 7.0 PBS containing 1 mg/ml Cyt c at 0.8 V. Inset: calibration plots illustrating the linear electrode response to H_2O_2 addition. (B). The chronoamperometry current-time curve of HRP/MWNT-IL electrode with successive addition of 0.06, 0.2, 0.5, 0.8, 1, 3, 5, 7, 9, 10, 15 and 20 μ M H_2O_2 to 0.10 M pH 7.0 PBS containing 2 mg/ml HRP at 0.8 V. Inset: calibration plots illustrating the linear electrode response to H_2O_2 addition.

3.3. Detecting H_2O_2 using Cyt c-MWNT-IL-GCE

Generally, the amperometric detection of H_2O_2 could be undertaken either by reduction or by oxidation. However, it is hard to remove oxygen completely from the buffer solution and every drop of H_2O_2 into the solution so that the reduction peak current could be attributed to the reduction of both H_2O_2 and oxygen. Therefore, we choose the oxidation potential for the detection of H_2O_2 in this paper.

Fig. 4A displayed the typical amperometric response for the fabricated Cyt c-MWNT-IL/GCE at an applied potential +0.8 V vs. SCE. A 0.1 M phosphate buffer at pH 7.0 has been used as the supporting electrolyte, and the amperometric response of the fabricated bioelectrode toward the detection of H_2O_2 has been carefully investigated by successive addition of H_2O_2 in PBS solution. Upon a potential step to the sensor in an unstirred system, the current-time behavior of an electrochemical system can be described by the Cottrell equation, and the faradaic current is expected to decay very



Scheme 2. Mechanism analysis to Cyt c or HRP in the presence of H_2O_2 .

slowly for long time. As shown in Fig. 4A, an increase in current with the concentration increase of H_2O_2 has been observed, and the calibration curve of the peak current versus the concentrations of H_2O_2 has been drawn as shown in the inset of Fig. 4A. It exhibits a linear range from 0.04 to 100 μM , and the linear regression equation was $i_p (\mu\text{A}) = 0.9521 + 0.5712c (\mu\text{M})$ with a correlation coefficient of 0.9980 ($n=5$). From the slope of 0.5712, the detection limit was estimated to be 0.013 μM at a signal-to-noise ratio of 3.

To further illustrate the universal appeal of this operation of oxidase-based amperometric biosensors, a similar procedure was employed for H_2O_2 detection as immobilized HRP on MWNT-IL/GCE. Fig. 4B reveals that the sensor response was linear between 0.06 and 20 μM with a correlation coefficient of 0.9976 ($n=5$).

For comparison, the analytical performances of the determination of H_2O_2 using different electrodes in this paper are listed in Fig. S-2. One can see that the linear response range with Cyt c or HRP immobilized on MWNT/IL electrode dramatically enhanced nearly 2 orders compared with bare GCE and MWNT-IL/GCE (data from Fig. S-3). The attractive advantage for Cyt c-MWNT-IL-GCE is attributed to the two points: (1) IL could detach the MWNTs from the bundles, accelerating the rate of electron transfer. (2) IL functionalization of CNTs provided an extra ionic affinity between MWNT and Cyt c, resulting in more electroactive sites of enzymes exposed on MWNTs-IL modified film. Thus, we proposed the mechanisms for H_2O_2 oxidation at the enzymes immobilized on MWNT/IL materials electrode in Scheme 2. Initially, Cyt c was immobilized onto the surface of MWNTs-IL/GCE, and IL functionalized CNTs make more electroactive sites of enzymes to be exposed on MWNT/IL materials. The synergic effect of MWNTs-IL might accelerate the electron transfer from the electroactive site of Cyt c, Fe^{III} , to the electrode. As Fe^{III} is electrochemically oxidized at MWNTs-IL electrode surface to produce an intermediate compound I ($\text{Fe}^{\text{IV}}=\text{O}$), the latter reacts with H_2O_2 in the solution, producing O_2 . Finally, compound I ($\text{Fe}^{\text{IV}}=\text{O}$) is reduced to form native Cyt c (Fe^{III}) again on the electrode surface.

3.4. Selectivity, reproducibility and stability of the H_2O_2 biosensor

One of the major challenges for the H_2O_2 biosensor is to eliminate the electrochemical response generated by some easily oxidizable endogenous interfering compounds such as ascorbic acid and dopamine. We have studied the selectivity of the present H_2O_2 biosensor against these possible interfering species through measuring the amperometric response to successive addition of physiological levels of various interfering species (40 μM AA(a), 40 μM DA(b), and 40 μM H_2O_2 (c)) at an applied potential of +0.8 V. As shown in Fig. S-4, the two interfering species (AA, DA) generated completely negligible current responses as compared to the current response of the same concentration for H_2O_2 , indicating a high selectivity for the as-prepared H_2O_2 biosensor. Furthermore, no significant interference can be observed for those general ions such as K^+ , Na^+ , Ca^{2+} , NH_4^+ , SO_4^{2-} , CO_3^{2-} , NO_3^- , Cl^- , PO_4^{3-} , at concentration 10-fold as high as that of H_2O_2 .

A relative standard deviation (RSD) of 2.8% was acquired when the present biosensor was repeated for ten successive measurements at a 5 μM H_2O_2 solution. RSD was 3.9% for five electrodes prepared in the same conditions. The stability of the biosensor was investigated by amperometric measurements in the presence of 50 μM H_2O_2 periodically. When not in use, it was stored under dry conditions at 4 $^\circ\text{C}$ in a refrigerator. The biosensor lost only 4.5% of the initial response after 1 week and maintained more than about 75% of the initial values after storage for more than 1 month. In addition, almost no decrease in the voltammetric response was observed when the biosensor was performed a 50 segments continuous scanning, implying that the enzyme electrode is stable in buffer solution.

4. Conclusion

In summary, a novel H_2O_2 biosensor based on IL-functionalized MWCNTs modified electrode has been fabricated successfully in

this paper. Investigation shows that the synergistic effect of IL and MWNTs not only provides a perfect microenvironment for Cyt c or HRP to retain its bioactivity but also exhibits a high surface area for enzyme immobilization. The as-prepared sensor displayed a series of excellent features such as good sensitivity and reproducibility, wide linear range, and low detection limit. Thus, it is also envisaged that the unique IL-functionalized MWNTs materials could provide a good biosensing platform. Moreover, combining the environment-friendly and designable ionic liquid with carbon nanotubes having excellent electrochemical characteristics may be a new idea for developing some novel and powerful biosensors.

Acknowledgments

The authors are most grateful to the Natural Science Foundation of China (nos. 21245004, 20875077, 20927004).

Appendix A. Supporting information

Supplementary data associated with this article can be found in the online version at <http://dx.doi.org/10.1016/j.talanta.2012.11.059>.

Reference

- [1] M. Ahmad, C. Pan, L. Gan, Z. Nawaz, J. Zhu, J. Phys. Chem. C 114 (2010) 243–250.
- [2] Y. Luo, H. Liu, Q. Rui, Y. Tian, Anal. Chem. 81 (2009) 3035–3041.
- [3] A.K.M. Kafi, G. Wu, A. Chen, Biosens. Bioelectron. 24 (2008) 566–571.
- [4] C. Shan, H. Yang, D. Han, Q. Zhang, A. Ivaska, L. Niu, Biosens. Bioelectron. 25 (2010) 1070–1074.
- [5] C.L. Xiang, Y.J. Zou, L.X. Sun, F. Xu, Electrochem. Commun. 10 (2008) 38–41.
- [6] T. Ito, M. Kunimatsu, S. Kaneko, Y. Hirabayashi, M. Soga, Y. Agawa, K. Suzuki, Talanta 99 (2012) 865–870.
- [7] X.J. Bian, K. Guo, L. Liao, J.J. Xiao, J.L. Kong, C. Ji, B.H. Liu, Talanta 99 (2012) 256–261.
- [8] Y. Mao, Y. Bao, W. Wang, Z.G. Li, F.H. Li, L. Niu, Talanta 85 (2011) 2106–2112.
- [9] Y. Kuwahara, T. Yamanishi, T. Kamegawa, K. Mori, H. Yamashita, J. Phys. Chem. B 115 (2011) 10335–10345.
- [10] I. Sumio, Nature 354 (1991) 56–58.
- [11] A. Hirsch, Angew. Chem. Int. Ed. 41 (2002) 1853–1859.
- [12] U.P. Sun, K. Fu, Y. Lin, W. Huang, Acc. Chem. Res. 35 (2002) 1096–1104.
- [13] S. Niyogi, M.A. Hamon, H. Hu, B. Zhao, P. Bhomwik, R. Sen, M.E. Itkis, R.C. Haddon, Acc. Chem. Res. 35 (2002) 1105–1113.
- [14] S. Banerjee, M.G.C. Kahn, S.S. Wong, Chem. Eur. J. 9 (2003) 1898–1908.
- [15] D. Tasis, N. Tagmatarchis, V. Georgakilas, M. Prato, Chem. Eur. J. 9 (2003) 4000–4008.
- [16] S. Banerjee, T. Hemraj-Benny, S.S. Wong, Adv. Mater. 17 (2005) 17–29.
- [17] M. Musameh, J. Wang, A. Merkoci, Y.H. Lin, Electrochem. Commun. 4 (2002) 743–746.
- [18] Z.H. Wang, J. Liu, Q.L. Liang, Y.M. Wang, G. Luo, Analyst 127 (2002) 653–658.
- [19] G.C. Zhao, Z.Z. Yin, L. Zhang, X.W. Wei, Electrochem. Commun. 7 (2005) 256–260.
- [20] S.W. Lee, S.K. Byeon, S. Chen, Y.S. Horn, Hammond Paula T., J. Am. Chem. Soc. 131 (2009) 671–679.
- [21] Y. Xiao, F. Patolsky, E. Katz, J.F. Hainfeld, I. Willner, Science 299 (2003) 1877–1881.
- [22] Y.J. Zhang, Y.F. Shen, D.X. Han, Z.J. Wang, J.X. Song, F. Li, L. Niu, Biosens. Bioelectron. 23 (2007) 438–443.
- [23] Y.Y. Ou, M.H. Huang, J. Phys. Chem. B 110 (2006) 2031–2036.
- [24] Z.W. Zhao, Z.P. Guo, J. Ding, D. Wexler, Z.F. Ma, D.Y. Zhang, Electrochem. Commun. 8 (2006) 245–250.
- [25] D. Tasis, N. Tagmatarchis, A. Bianco, M. Prato, Chem. Rev. 106 (2006) 1105–1136.
- [26] M.A. Hamon, J. Chen, H. Hu, Y.S. Chen, M.E. Itkis, A.M. Rao, P.C. Eklund, R.C. Haddon, Adv. Mater. 11 (1999) 834–840.
- [27] Y.J. Zhang, Y.F. Shen, J.H. Yuan, D.X. Han, Z.J. Wang, Q.X. Zhang, L. Niu, Angew. Chem. Int. Ed. 45 (2006) 5867–5870.
- [28] T. Welton, Chem. Rev. 99 (1999) 2071–2083.
- [29] S.F. Ding, W. Wei, G.C. Zhao, Electrochem. Commun. 9 (2007) 2202–2206.
- [30] Y.T. Shieh, G.L. Liu, H.H. Wu, C. Lee, Carbon 45 (2007) 1880–1890.
- [31] C. Lau, Y. Mi, Polymer 43 (2002) 823–829.
- [32] M.J. Park, J.K. Lee, B.S. Lee, Y.W. Lee, I.S. Choi, S.G. Lee, Chem. Mater. 18 (2006) 1546–1551.
- [33] L. Li, C.H. Bu, Y.J. Zhang, J. Du, X.Q. Lu, X.H. Liu, Electrochim. Acta 58 (2011) 105–111.